ISSN (Print) 1226-1750
ISSN (Online) 2233-6656
Journal of Magnetics 24(1), 142-148 (2019) https://doi.org/10.4283/JMAG.2019.24.1.142

Design of Dual Skewed Rotor in Cage Induction Motor for Reducing Synchronous Parasitic Torque

Wei Xu[1], Xiaohua Bao[1]*, Sheng Xu[2], and Zechen Li[1]

[1]*School of Electrical Engineering and Automation, Hefei University of Technology, Hefei 230009, China*
[2]*School of Management, Hefei University of Technology, Hefei 230009, China*

(Received 24 June 2018, Received in final form 24 December 2018, Accepted 27 December 2018)

Dual skewed rotor is an improved skewed rotor pattern in suppressing the slot harmonics. However, in order to lessen synchronous parasitic torque, the relevant structural parameters should be modified for different slot combinations. According to the unified expressions of magnetic flux densities, the general harmonic torque could be calculated with the virtual displacement method. Then, the synchronous torque ratio is proposed to reflect the effect of synchronous parasitic torque on the starting torque. Under the premise of the assumed parameter range, the rotor type and minimized skewed angle are determined for three kinds of slot combinations. The normal skewed rotor could be seen as a special topology of dual skewed rotor. Finally, the validity of designing process is verified by the comparison of simulation study and experimental results.

Keywords : dual skewed rotor, synchronous parasitic torque, slot combination, optimization design

1. Introduction

The skewed cage rotor induction motor has a positive influence on weakening the slot harmonics, thus several electromagnetic characteristics like starting torque could be improved [1]. Based on the theory of regular skewed rotor, dual skewed rotor is introduced to lessen electromagnetic noise by intensifying the skewing effect [2]. However, the skewed rotor also brings some negative impacts on other performances. Skewing the rotor alters the balance of losses and results in the increased total losses in large induction motors. The extra losses are partly originated form the inter-bar current which is promoted by the skew [3]. Even with an insulated cage rotor, the skewing also lower the efficiency. The harmonic loss is in proportion to the skewed angle for any value of inter-bar resistance [4]. Thus the skewed angle should be small as much as possible under the premise of satisfaction of main requirements. As the skewed angle should not be bigger than necessary, there exists an optimal value for certain performance of the machine [5]. This principle also fits to the dual skewed cage rotor induction motor in which the decreased skewed angle is relevant to a higher fundamental torque [6].

Normally, the stator and rotor slot combination should be carefully selected, especially for the purpose of avoiding the torque disturbance caused by the parasitic torques [1]. The smooth torque-slip curve in classic model neglects the spatial harmonic and skin effect. But a torque dip at large slips in motoring regime and a notable torque increase in barking regime exist on the real project applications [7]. Several presented analytical models take harmonic parasitic torques into account by estimating the distribution of magnetomotive force (MMF) [8, 9]. However, certain special cases with inappropriate slot combinations like equivalent slot number are discarded in general owing to the terrible starting torque.

Aiming at the unsolved parasitic torque problem in normal skewed-rotor induction motor, dual skewed rotor is applied to suppress the harmonic torque. The rotor pattern and minimized skewed angle would be determined for different slot combinations. The designing process of dual skewed rotor is based on the proposed synchronous torque ratio as shown in Fig. 1. Cause for the minor impact on lowering the synchronous parasitic torque, the normal skewed rotor is regarded as the initial rotor type. The value of skewed angle is gradually decreased from

*Corresponding author: Tel: +86-0551-62905883
Fax: +86-0551-62905883, e-mail: sukz@ustc.edu

This paper was presented at the IcAUMS2018, Jeju, Korea, June 3-7, 2018.

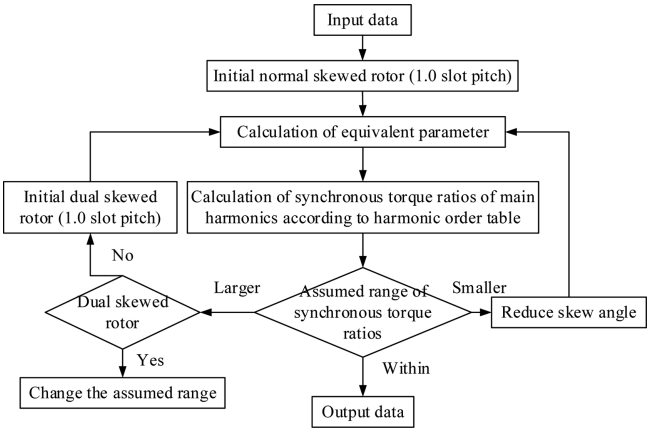

Fig. 1. Flowchart of skewed rotor design process.

the 1.0 rotor slot pitch which is always considered as a routine skewed angle [1]. Although different angle combinations could result in the identical skewing effect [6], the stagger angle here is constantly equal to half a rotor slot pitch for the rapidity of calculation.

This paper aims at reducing the synchronous parasitic torque by ascertaining the suitable skewed rotor type and minimized skewed angle for different slot combinations. The distribution of simplified rotor magnetic flux density in dual skewed rotor is achieved firstly. Then the relation between synchronous parasitic torque and slot combination is researched on with the harmonic order table. The synchronous torque ratio is proposed to represent the specific torque component in the starting torque. Finally, the analysis methodology is verified by the contrast models with 3D FEM and experiment.

2. Slot Harmonic Magnetic Field

In order to simplify the process of calculation, the air-gap length is assumed to be uniform in this paper. Thus the flux density wouldn't be affected by harmonic permeance. Regardless of the skewing effect, the expressions of stator and rotor magnetic flux densities are similar to each other. Relative to the corresponding coordinate systems, the stator and rotor harmonic magnetic flux densities in straight-slot induction motor are expressed respectively as [6]

$$b_{\nu b}(\theta,t) = B_{\nu b}\cos(\nu_b\theta - \omega_1 t - \varphi_{\nu b}) \tag{1}$$

$$b_{\mu a}(\theta,t) = B_{\mu a}\cos\left[\mu_a\theta_r - \left(\omega_1 - \frac{\nu_a}{p}\omega_r\right)t - \varphi_{\mu a}\right] \tag{2}$$

where $B_{\nu b}$ and $B_{\mu a}$ are separately the amplitudes of stator and rotor harmonic flux densities, $\varphi_{\nu b}$ and $\varphi_{\mu a}$ are the initial phase angles of corresponding harmonics, ω_1 is the angular frequency of power supply and ω_r is the electrical angular velocity of rotor.

Particularly, the rotor harmonic magnetic field $b_{\mu a}$ is originally produced by the ν_a^{th} stator harmonic. The subscript of the symbol represents the pole pairs of slot harmonics, to be specific, stator slot harmonic ν_b and rotor slot harmonic μ_a are expressed respectively as [10]

$$\nu_b = k_{1b}Z_1 + p \tag{3}$$

$$\mu_a = k_{2a}Z_2 + \nu_a \tag{4}$$

where p is the number of pole pairs, Z_1 and Z_2 are separately the number of stator slots and rotor slots. k_{1b} and k_{2a} are equal to ± 1, ± 2, $\pm 3\ldots$ where the "$\pm$" represents the resolving direction of harmonic waves.

Within an assumed interval time Δt, the rotor rotates with a certain mechanical angle $\Delta\theta_r$. According to the expression of rotor harmonic (2), the phase of rotor time harmonic $b_{\mu a}$ increases by an angle $(\omega_1 - \nu_a\omega_r/p)\Delta t$. From another perspective, while the rotor is considered to be still, the stator rotates equivalently with an equal angle in the inverse direction. The corresponding ν_a^{th} stator spatial harmonic is changed with an electrical angle $\Delta\theta_r\nu_a$. Thus, the phase difference and time difference could be related as

$$\Delta\theta_r\nu_a = \left(\omega_1 - \frac{\nu_a}{p}\omega_r\right)\Delta t \tag{5}$$

By substituting equation (5) into equation (2), the rotor spatial harmonic magnetic field at the moment of $\Delta t + t$ could be simplified as

$$b'_{\mu a} = B_{\mu a}\cos\left[\mu_a\theta_r - \left(\omega_1 - \frac{\nu_a}{p}\omega_r\right)t + k_{2a}Z_2\Delta\theta_r - \varphi_{\mu a}\right] \tag{6}$$

The period of rotor spatial harmonic $T_r = 2\pi/(Z_2k_{2a})$ could be attained by comparing equations (2) with (6). Obviously, the least common multiple of the period of rotor harmonic is equal to one rotor slot pitch t_2. The periodicity of spatial harmonics wouldn't be altered by the skewed rotor pattern.

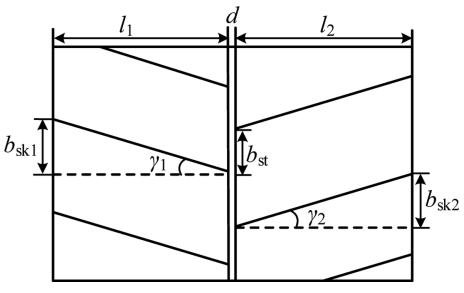

Fig. 2. Simplified planar model of dual skewed rotor.

The classical symmetric structure of dual skewed rotor is applied in this paper to offset the axial electromagnetic force [6]. The simplified planar model is shown in Fig. 2. The lengths of skewed bars l_1, l_2 and the skewed distances b_{sk1}, b_{sk2} are equal with each other respectively ($l_1 = l_2 = l$, $b_{sk1} = b_{sk2} = b_{sk}$). Two parts of rotor bars are connected by intermediate ring, the axial length of which is marked as d. b_{st} is the stagger distance between the two skewed bars. The skewed angle and stagger angle are respectively the mechanical angles of corresponding distance.

The phase angle of rotor slot harmonic is always behind than that of stator slot harmonic. In order to unify the rotor magnetic fields into the stator static coordinate system, the rotor mechanical angle θ_r should be translated into the stator angle coordinate θ.

$$\theta_r = \theta - \frac{\omega_r}{p}t \tag{7}$$

The induced rotor current in skewed bar generates the rotor MMFs, which are varied gradually along the direction of shaft. The skewing effect could be reflected by a phase difference varied with the spatial axial position z_1, z_2 in the unified coordinate system. By substituting equation (7) into (2), the rotor harmonic magnetic flux densities in dual skewed rotor could be rewritten into two parts as

$$b_{\mu a1} = B_{\mu a1}\cos\left(\mu_a\theta - \omega_\mu t - \mu_a\frac{b_{sk1}z_1}{Rl_1} - \varphi_{\mu a}\right) \tag{8}$$

$$b_{\mu a2} = B_{\mu a2}\cos\left(\mu_a\theta - \omega_\mu t - \mu_a\frac{b_{sk2}z_2}{Rl_2} - \mu_a\frac{b_{st}}{R} - \varphi_{\mu a}\right) \tag{9}$$

where

$$\omega_\mu = \left[1 + \frac{k_{2a}Z_2}{p}(1-s)\right]\omega_1 \tag{10}$$

ω_μ is the angular frequency of rotor harmonic magnetic fields in the stator static coordinate system, s is the slip ratio, R is the rotor outer radius. Obviously, different rotor slot numbers would result in the different harmonic angular frequencies even with the same slip ratio.

3. Synchronous Parasitic Torque

3.1. Harmonic electromagnetic torque

Considering the symmetrical structure of the analyzed dual skewed rotor, the first part of rotor magnetic field is illustrated as an example. The electromagnetic torque is calculated by differentiating the air-gap magnetic energy with respect to a virtual electrical displacement Δ [5]. In the stator static coordinate system, the arbitrary electrical angle Δ could be represented as the relative position of rotor magnetic fields. With the equations (1) and (8), the harmonic electromagnetic toque could be expressed as

$$\begin{aligned} T_{\nu\mu1}(\theta,t) &= -\frac{\partial}{\partial\Delta}\int_V \frac{(b_{\nu b}+b_{\mu a1})^2}{2\mu_0}\,dv \\ &= -\frac{gr}{\mu_0}\int_{-l_1/2}^{l_1/2}\int_0^{2\pi}(b_{\nu b}+b_{\mu a1})\frac{\partial b_{\mu a1}}{\partial\Delta}\,dz_1 d\theta \end{aligned} \tag{11}$$

where g is the air-gap axial length, r is the air-gap average radius and μ_0 is the permeability of vacuum.

The integral value of harmonic torque isn't equal to zero in a circumferential period (2π) when the absolute values of pole pairs are equal with each other ($|\nu_b| = |\mu_a|$). Thus the simplified harmonic torque could be expressed as

$$T_{\mu a1}(t) = -\mu_a\frac{\pi gr}{\mu_0}B_{\nu b}B_{\mu a1}\int_{-l_1/2}^{l_1/2}\sin(t,z_1)dz_1 \tag{12}$$

where

$$\sin(t,z_1) = (\omega_\mu \mp \omega_1)t + \mu_a\frac{b_{sk1}z_1}{Rl_1} + (\varphi_{\mu a} - \varphi_{\nu b}) \tag{13}$$

Harmonic electromagnetic torque is apparently changed with the rotation time t except when the compound angular frequency is satisfied with $\omega_\mu \mp \omega_1 = 0$. The symbol "$\mp$" depends on the rotation direction of the harmonic magnetic field. Both the conditions of pole pairs and angular frequency are satisfied, the relevant harmonic torque is just the constant synchronous parasitic torque. On this occasion, the generating rotation velocity n_μ is acquired as

$$n_\mu = 0, \text{ when } \nu_b = \mu_a \tag{14}$$

$$n_\mu = -\frac{120f}{k_{2a}Z_2}, \text{ when } \nu_b = -\mu_a \tag{15}$$

Another part of harmonic torque could be calculated with the same method. As for the symmetrical structure of dual skewed rotor, the relevant electromagnetic parameters are similar to each other, for instance, the amplitudes of rotor harmonic flux density $B_{\mu a1} = B_{\mu a2} = B_{\mu a}$. In consequence, the final compound synchronous parasitic torque is

$$T_{\mu a} = -\frac{2l\pi gr\mu_a}{\mu_0}B_{\nu b}B_{\mu a}k_{ds\mu}\sin\left(\varphi_{\mu a} - \varphi_{\nu b} + \mu_a\frac{b_{st}}{2R}\right) \tag{16}$$

where

$$k_{ds\mu} = \frac{\sin\left(\mu_a\frac{b_{sk}}{2R}\right)\cos\left(\frac{\mu_a b_{st}}{2R}\right)}{\mu_a\frac{b_{sk}}{2R}} \tag{17}$$

$k_{ds\mu}$ is the harmonic double-skewing factor.

The phase angle ($\varphi_{\mu a}$–$\varphi_{\nu b}$) in equation (16) depends on the phase relation between the generating stator and rotor harmonics. The amplitude of synchronous parasitic torque is obviously a period function changed with operation position. What's more, the normal single skewed rotor could be regarded as a special topology of dual skewed rotor. The skewing effect on the synchronous torque could be reflected by the double-skewing factor.

3.2 Stator and rotor slot combination

The value of harmonic electromagnetic torque is directly proportional to the amplitudes of corresponding harmonic flux densities. According to the definition of current linkage, the stator flux density is inverse proportion to the harmonic order ν and direct proportion to the harmonic winding factor $k_{w\nu}$[1]. The ratio of rotor fundamental and harmonic flux densities in the modified equivalent circuit considering the harmonics is reduced to

$$\frac{B_\mu}{B_p}=\frac{pI'_{2\nu}}{\mu_a I'_{2p}}\approx\frac{X_m+X'_{21}}{R'_{21}}\frac{p^2k^2_{w\nu}}{\nu_a\mu_a k^2_{w1}} \tag{18}$$

where X_m is the magnetizing reactance, X'_{21} and R'_{21} are separately the rotor reactance and rotor resistance. k_{w1} and $k_{w\nu}$ are separately the winding factors of the fundamental order p and harmonic order ν.

The synchronous parasitic torque is a sine function varied with the angle variable ($\varphi_{\mu a}$–$\varphi_{\nu b}$). Obviously, there exists a worst situation when the synchronous torque is just equal to the maximum value. Thus the ratio of maximum synchronous torque and fundamental torque could be referred in the starting process.

$$k_{st}=\frac{M_\mu}{M_p}\approx\frac{X_m+X'_{21}}{R'_{21}}\frac{p^2k^3_{w\nu}}{\nu_a\mu_a k^3_{w1}}\frac{k_{ds\mu}}{k_{dsp}} \tag{19}$$

The synchronous parasitic torque ratio k_{st} describes the effect of synchronous torque on the starting torque. In order to have a satisfying start-up characteristic, the value of maximum synchronous torque ratio must be smaller than one. Since more than one harmonics meet the generating conditions, take the case of four-pole induction motor with 24-24 slot combination, for instance, the relation of harmonic order could be reflected by the harmonic order table as shown in Table 1.

When the $\mu_a{}^{th}$ rotor slot harmonic originates from the $\nu_a{}^{th}$ stator harmonic, this mathematic relation could be reflected in any single line in Table 1. However, according to the definition of synchronous parasitic torque, the same values of related harmonic order should be in different lines. In the situation of normal induction motor, slot harmonics are hard to be eliminated, thus the main synchronous parasitic torque are generated by the first slot harmonics –22 and 26.

Table 1. Pole pairs of main harmonics for 24-24 combination

Stator harmonics		Rotor slot harmonics $\mu_a = k_{2a}Z_2 + \nu_a$				
$\nu_a = (6k_1 + 1)p$		k_{2a}				
k_1	ν_a	0	–1	1	–2	2
0	2	2	–22	26	–46	50
–1	–10	–10	–34	14	–58	38
1	14	14	–10	38	–34	62
–2	–22	–22	–46	2	–70	26
2	26	26	2	50	–22	74
–3	–34	–34	–58	–10	–82	14
3	38	38	14	62	–10	86
–4	–46	–46	–70	–22	–94	2
4	50	50	26	74	2	98

Table 2. Partial features of synchronous parasitic torque for different slot combinations.

Symbol	Quantity	Value		
Z_1-Z_2	Slot combina tion	24-24	24-26	24-28
μ_a	Pole pairs of slot harmonic	–22, 26	–50	–22, 26
n_μ	Generating velocity	0	115.4	214.3
T_{rs}	Periodicity	t_2	t_2/2	t_2

The generating velocity of corresponding synchronous parasitic torque could be calculated with equation (14) or (15). The spatial period of the parasitic torque is same as that of relevant rotor spatial harmonic according to the previous discussions. Similar conclusions could be attained for three kinds of slot combinations as shown in Table 2. The rotor slot number is remarkably larger than stator slot number, only in this way, the value of generating velocity of synchronous parasitic torque is larger than zero.

4. Design Process of Dual Skewed Rotor

4.1. Straight-slot rotor

The amplitude of harmonic electromagnetic torque could be depressed by skewed rotor, but the basic features of general electromagnetic torque are independent to the type of skewed rotor. Three kinds of induction motors with straight-slot rotor are analyzed with two dimensional finite element method (2D FEM). The number of rotor slot as the only variable parameter is separately 24, 26 and 28. Other remained parameters of three motor models are completely identical with each other as shown in Table 3.

Table 3. Main parameters of cage induction motor.

Symbol	Quantity	Value
p	Number of pole pairs	2
P	Rated power (kW)	1.5
U	Rated voltage (V)	380
f	Rated frequency (Hz)	50
Z_1	Number of stator slots	36
D_1	Stator outer diameter (mm)	135
D_2	Rotor outer diameter (mm)	85.5
L	Core length (mm)	115

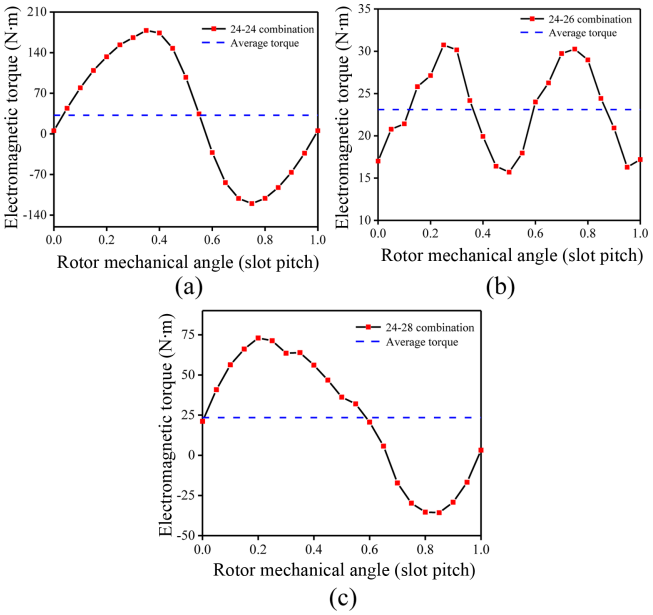

Fig. 3. (Color online) Electromagnetic torque of cage induction motor with straight-slot rotor (a) 24-24 slot combination (b) 24-26 slot combination (c) 24-28 slot combination.

Those contrastive models are operated at the specific velocity shown in Table 2. The current source excitation should be adjusted according to the current-speed curve. The total electromagnetic torque varied with the rotor mechanical position are shown in Fig. 3.

The waveform period of total electromagnetic torque in Fig. 3 is separately equal to that of predicted synchronous torque. The maximum torque is far more than the average torque, which means that synchronous parasitic torque is the chief component. The average electromagnetic torque could be nearly seen as the fundamental torque, which is almost constant within the range of one slot pitch. The average torque for three kinds of slot combinations are respectively 32.2 N·m, 23.1 N·m and 23.5 N·m. But the minimum torque could not meet the least principle of start-up characteristic. The rotor type and skewed angle should be modified to lessen the synchronous parasitic torques.

4.2. Dual skewed rotor

The primary harmonics generating the synchronous parasitic torques should be attenuated by changing the angle parameter in the double-skewing factor. Actually, when the stagger angle is equal to zero, the double-skewing factor is just the skewing factor of normal skewed rotor. Utilizing the circular program in Fig. 1, the range of the absolute value of synchronous torque ratio here is assumed as (0.2-0.3). The synchronous torque ratios of dominant orders are calculated continuously until the maximum parameter meets the assumed range. The comparison of synchronous torque ratios between the original straight-slot rotor and adopted skewed rotor is shown in Table 4.

One rotor slot pitch is selected as an essential numerical unit of skewed angle. Final results show that dual skewed rotor (DS) apply to the higher proportion of synchronous parasitic torque, while normal skewed rotor (NS) has a relatively weak effect. After substituting the optimized skewed rotor, synchronous parasitic torques have a sharp decrease no matter which component plays the leading

Table 4. Partial synchronous parasitic torque ratios for different slot combinations.

Slot combination	Rotor slot harmonic	Pole pairs	Straight-slot rotor	Skewed rotor	
24-24	First	–22	–4.91	1.0 DS	0.06
		26	–4.15		0.04
	Second	–46	2.35		0.11
		50	2.16		0.09
24-26	Second	–50	2.19	0.9 NS	–0.30
		–74	–0.13		–0.02
24-28	First	22	–0.19	0.9 DS	–0.03
		–26	–4.06		–0.10
	Second	46	0.46		0.10

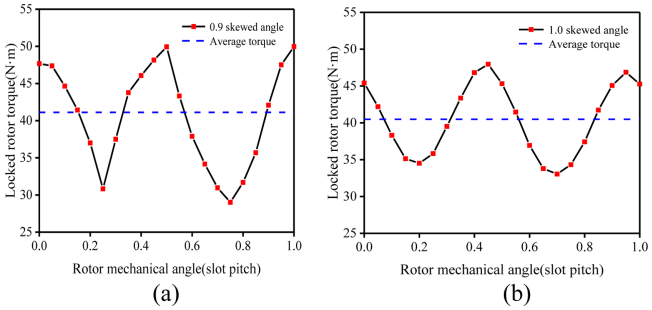

Fig. 4. (Color online) Simulated locked-rotor torque for 24-24 dual skewed rotor (a) 0.9 skewed angle (b) 1.0 skewed angle.

role. The synchronous parasitic torques produced by first slot harmonics apparently become the minor component.

In order to further verify the calculated results, take the 24-24 slot combination as an example, two kinds of models with 0.9 DS and 1.0 DS are simulated with 3D finite element method (3D FEM). The locked rotor torque versus rotor position curve is shown in Fig. 5.

The primary synchronous parasitic torques for 24-24 slot combination just happen when the rotation speed is equal to zero. After applying the dual skewed rotor, the period of locked-rotor torque turns into the half of the original period. This transformation shows that first rotor slot harmonic is hardly remained, while the second slot harmonic is the dominant source of synchronous parasitic torque. The numerical relation of synchronous torques can be indicated from the proposed synchronous torque ratio. The latter case is better for the sufficient starting torque, although the average torque is reduced slightly.

4.3. Experimental verification

The prototype motors with two kinds of dual skewed rotor are manufactured to verify the simulated results. Since the torque spikes and dips are hard to be directly measured, 24-24 slot combination is selected like the previous contrast models. The relevant skewed angles are 0.9 and 1.0 rotor slot pitch. Other parameters of two prototype motors are identical with each other. The closed-slot type is chosen as the rotor slot, thus the surface insulation covers the shape of skewed bar as shown in Fig. 6(a). The rotor and shaft are fixed by the arm of force, which should be horizontal to measure the force translating into the locked-rotor torque. The whole built experimental platform is shown in Fig. 6(b).

The stator could rotate in the processed dial to change the relative position between stator and rotor. The locked-rotor torque are tested at specific circumferential angles 0, 14, 28, 42, 56, 70, 84 etc. Since one slot pitch is a position period, the angle coordinate could be converted into 0~25 relative degree. The locked-rotor torque varies

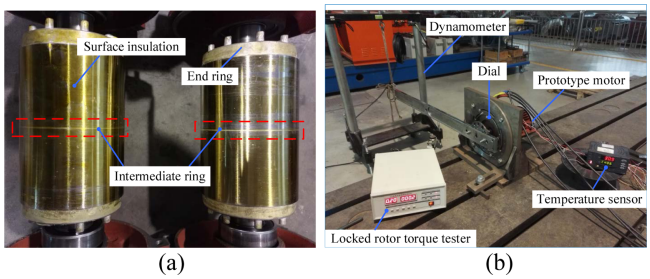

(a) (b)

Fig. 5. (Color online) Measurement of locked-rotor torque for prototype motors with 24-24 slot combination (a) dual skewed rotor (b) experimental platform.

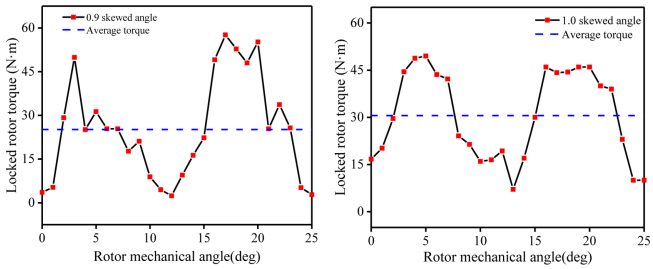

(a) (b)

Fig. 6. (Color online) Measured locked-rotor torque for 24-24 dual skewed rotor (a) 0.9 skewed angle (b) 1.0 skewed angle.

with the rotor mechanical angle is as shown in Fig. 6.

The waveforms of locked-rotor torque are generally similar, while the period of locked-rotor torque approaches to a half rotor slot pitch. Although the values of maximum torque are close to each other, the minimum torque for 0.9 skewed rotor is 2.7 Nm while for 1.0 skewed rotor is 10 Nm. The latter prototype motor is obviously better than the former motor, dual skewed rotor with 1.0 skewed angle is suggested to be applied for the situation with 24-24 slot combination.

5. Conclusion

Dual skewed rotor is helpful to weaken the synchronous parasitic torque in the starting process. According to the percentage of synchronous parasitic torque, the relevant design strategy should be varied with slot combination. The range of absolute value of synchronous torque ratio is assumed as (0.2~0.3) in this paper. The calculated results show that 1.0 DS suits for 24-24 combination, while 0.9 NS suits for 24-26 combination and 0.9 DS suits for 24-28 combination. The stagger distance of dual skewed rotor is invariably equal to half a rotor slot pitch. Two prototype motors with dual skewed rotor are manufactured to measure the locked-rotor torque. The validity of the design strategy is verified by comparing the results between simulation and experiment. As for the 24-24 combination prototype motor, the starting torque ratio range is improved into 1.5~5.0 by using the optimized-designed skewed rotor.

Acknowledgements

This work was undertaken in part by the National Natural Science Foundation of China (No. 51677051).

References

[1] J. Pyrhonen, T. Jokinen, and V. Hrabovcova, Design of

Rotating Electrical Machines, Wiley, New York (2010) pp 250-253.
[2] L. Wang, X. Bao, C. Di, and Y. Zhou, IEEE Trans. Magn. **52**, 7 (2016).
[3] C. I. McClay and S. Williamson, IEEE Trans. Ind. Appl. **36**, 1563 (2000).
[4] S. Williamson and A. C. Smith, International Conference on Power Electronics (2002) pp 369-374.
[5] D. Strbac and R. Gottkehaskamp, IKMT 2015; 10. ETG/ GMM-Symposium Innovative small Drives and Micro-Motor Systems (2015) pp 1-7.
[6] W. Xu, X. Bao, C. Di, L. Wang, and Y. Chen, IEEE Trans. Magn. **53**, 11 (2017).
[7] L. Monjo, F. Córcoles, and J. Pedra, IET Electr. Power Appl. **9**, 377 (2015).
[8] H. R. Cha, C. H. Yun, T. U. Jung, H. M. Kim, J. C. Kim, S. H. Baek, and K. H. Kim, 32nd Annual Conference on IEEE Industrial Electronics (2006) pp 1018-1022.
[9] K. Yamazaki, Y. Haruishi, and T. Ara, IEEE Trans. Magn. **40**, 778 (2004).
[10] L. Wang, X. Bao, C. Di, Y. Zhou, and Q. Lu, IET Electric. Power Appl. **11**, 1357 (2017).